Valence tautomerism and dynamic behavior of cobalt complexes with an anthracene-containing dioxolene ligand

Koichi Katayama, Masakazu Hirotsu,* Isamu Kinoshita, and Yoshio Teki*

Division of Molecular Materials Science, Graduate School of Science,
Osaka City University
3-3-138 Sugimoto, Sumiyoshi-ku, Osaka 558-8585 (Japan)
E-mail: mhiro@sci.osaka-cu.ac.jp; teki@sci.osaka-cu.ac.jp

Supplementary Information Data

IR spectra of **1**-**4**, ^{1}H NMR spectra of **1**-**4**, (i) and H_2L, variable temperature ^{1}H NMR spectra of **1**-**4**, Eyring plots of **1** and **2**, LIVT measurements of complexes **2** and **3**, and TRESR spectrum of H_2L are presented as supplementary information.

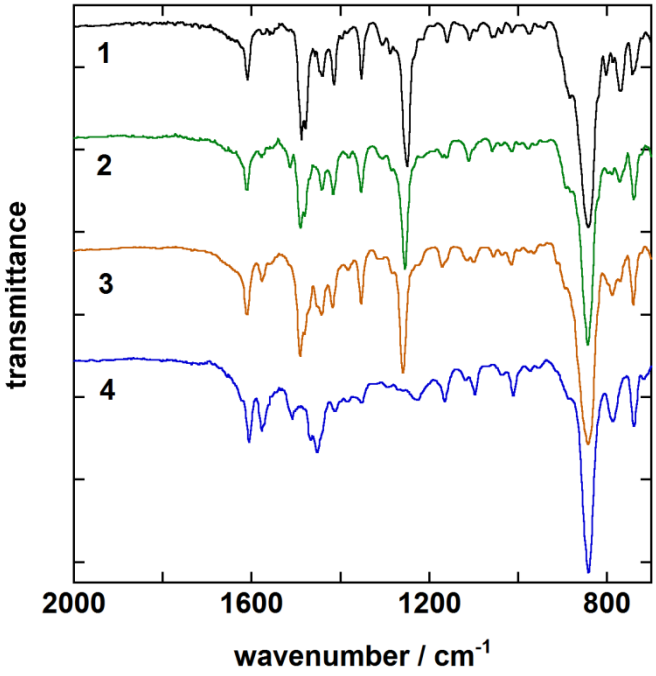

Figure S1. IR spectra of complexes **1**-**4** at room temperature.

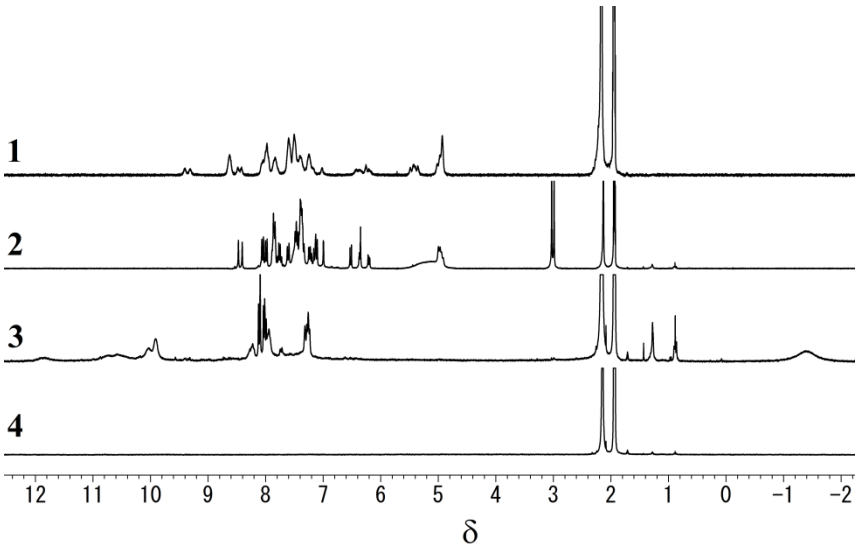

Figure S2. ^{1}H NMR spectra (300 MHz) of complexes **1**-**4** at room temperature in acetonitrile-d_3.

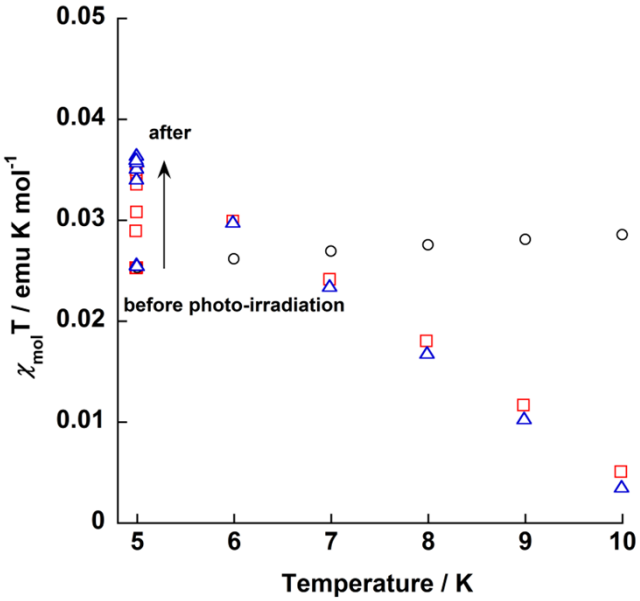

Figure S3. Temperature dependence of magnetic susceptibilities of complex **2**, the bulk powder sample (○), after irradiation with 355 nm light (□) and 532 nm light (△). The χ_MT values of the thin samples at 5 K before photo-irradiation were corrected by using that of the bulk powder sample at 5 K. The values after photo-irradiation are lower than those of the bulk powder sample above 7 K because the susceptibility data were not corrected for the diamagnetism of the tape.

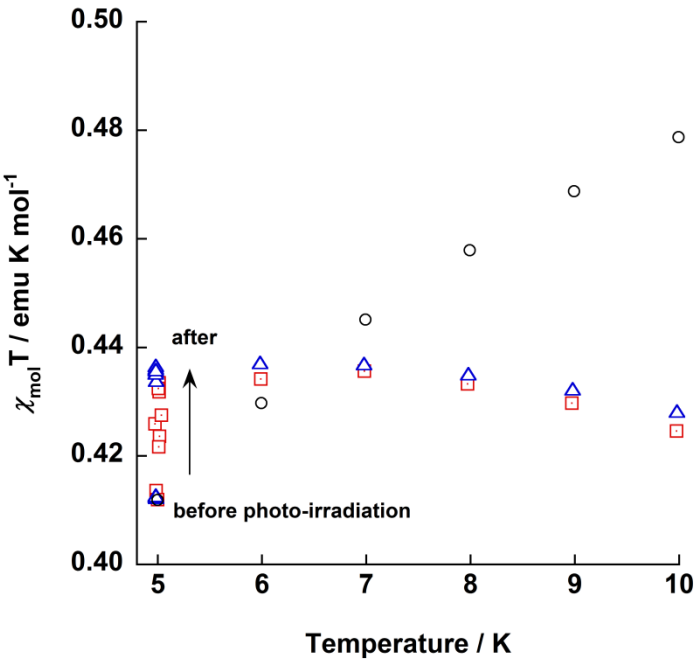

Figure S4. Temperature dependence of magnetic susceptibilities of complex **3**, the bulk powder sample (○), after photo-irradiation 355 nm (□) and 532 nm (△). The χ_MT values of the thin samples at 5 K before photo-irradiation were corrected by using that of the bulk powder sample at 5 K. The values after photo-irradiation are lower than those of the bulk powder sample above 7 K because the susceptibility data were not corrected for the diamagnetism of the tape.

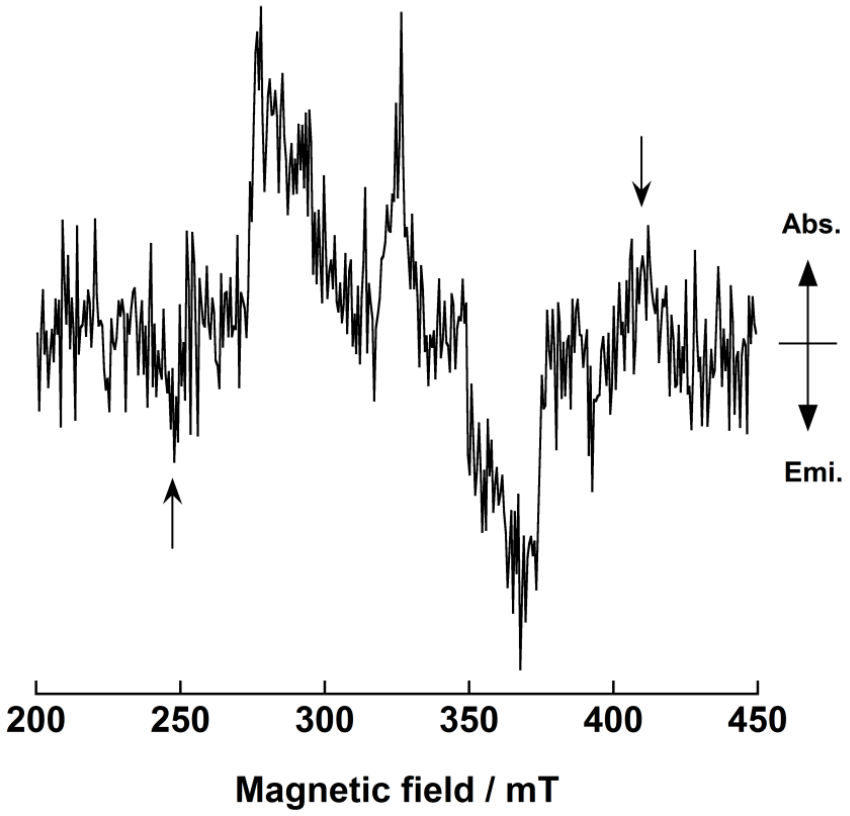

Figure S5. TRESR spectrum of H_2L at 30 K in a 2-Me-THF glass matrix at 0.5 μs. "Abs." and "Emi." denote the absorption and emission of microwave. The signals were observed in the range of 250 to 420 mT. The deduced *D* value is about 0.07 cm^{-1}, which is similar to that of anthracene (0.0710 cm^{-1}).

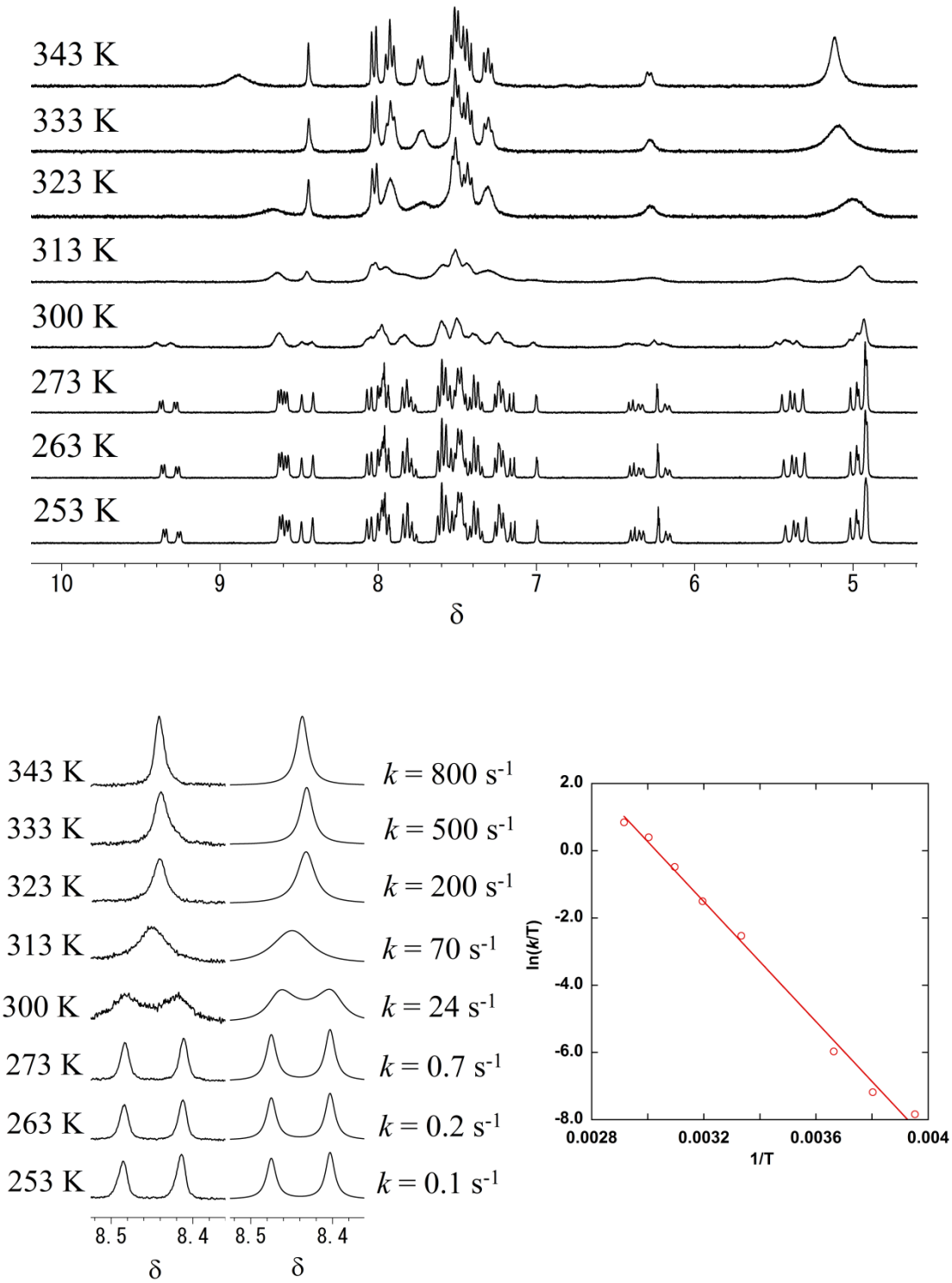

Figure S6. Observed (left) and simulated (middle) signals of 10-H proton of the anthracene ring in variable temperature ^{1}H NMR spectra of **1** in acetonitrile-d_3. Eyring plot of complex **1** (right): $\ln(k/T) = -\Delta H^{\ddagger}/(RT) + \ln(k_B/h) + \Delta S^{\ddagger}/R$; k, rate constant; T, temperature; R, gas constant; k_B, Boltzmann constant; h, Planck constant; $\Delta H^{\ddagger}$, activation enthalpy; $\Delta S^{\ddagger}$, activation entropy.

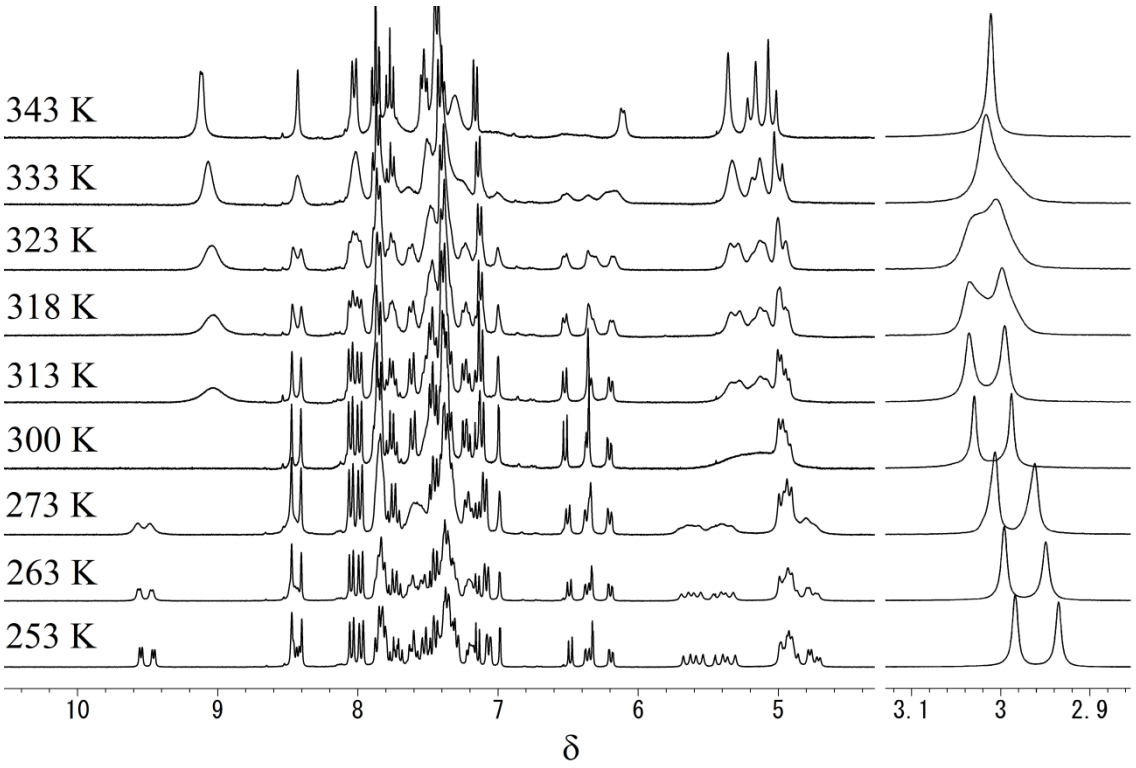

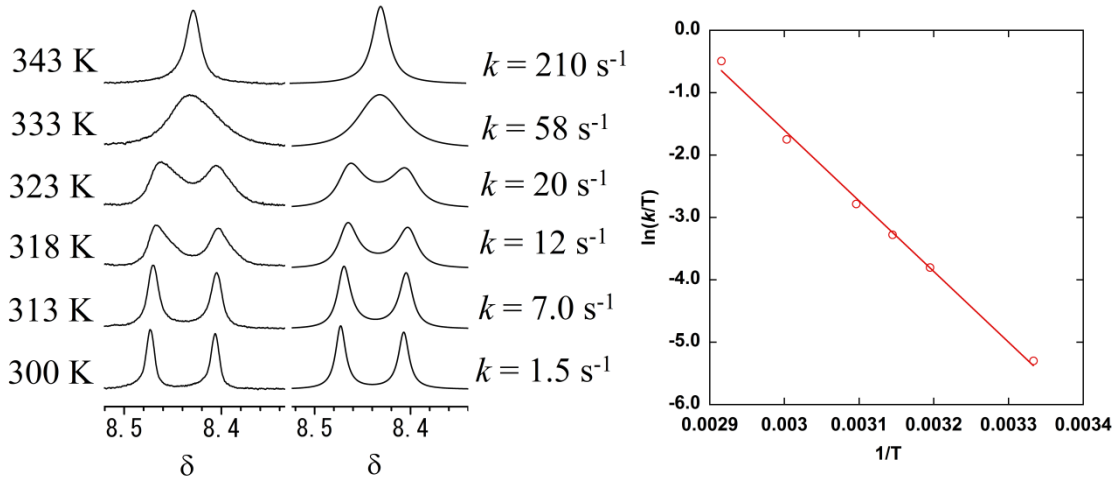

Figure S7. Observed (left) and simulated (middle) signals of 10-H proton of the anthracene ring in variable temperature ^{1}H NMR spectra of **2** in acetonitrile-d_3. Eyring plot of complex **2** (right): $\ln(k/T) = -\Delta H^{\ddagger}/(RT) + \ln(k_B/h) + \Delta S^{\ddagger}/R$; k, rate constant; T, temperature; R, gas constant; k_B, Boltzmann constant; h, Planck constant; $\Delta H^{\ddagger}$, activation enthalpy; $\Delta S^{\ddagger}$, activation entropy.

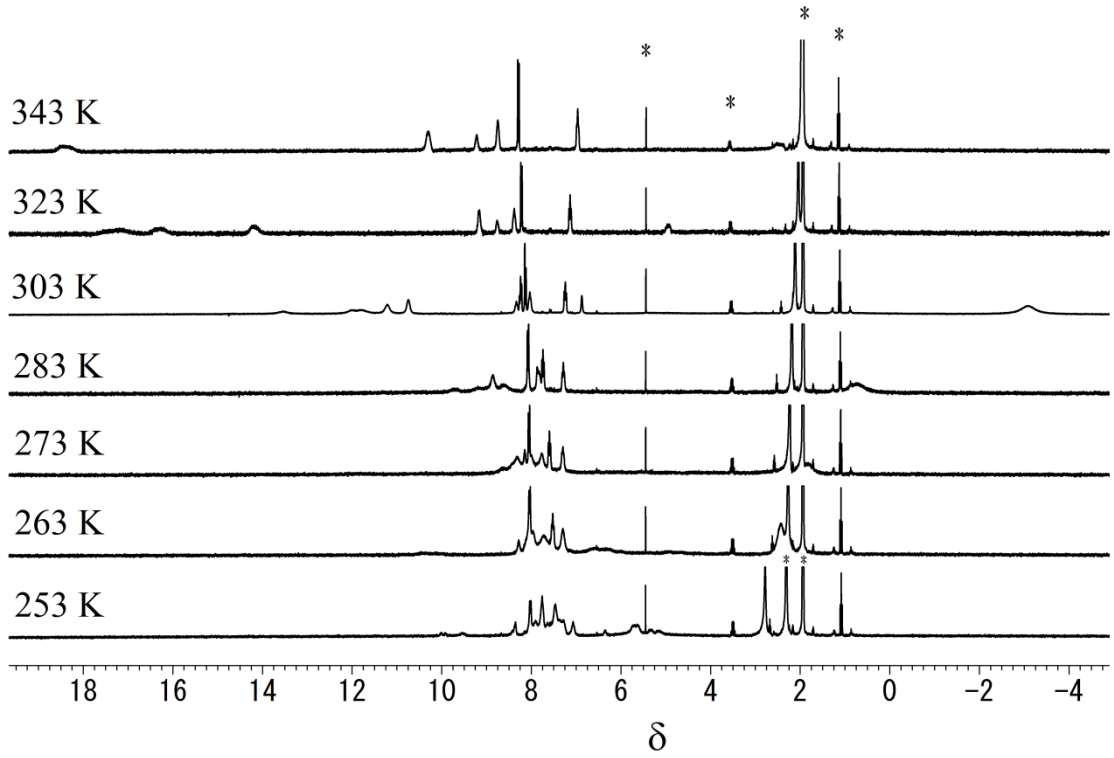

Figure S8. Variable temperature ^{1}H NMR spectra (300 MHz) of complex **3** in acetonitrile-d_3. Residual solvent signals are marked with an asterisk.

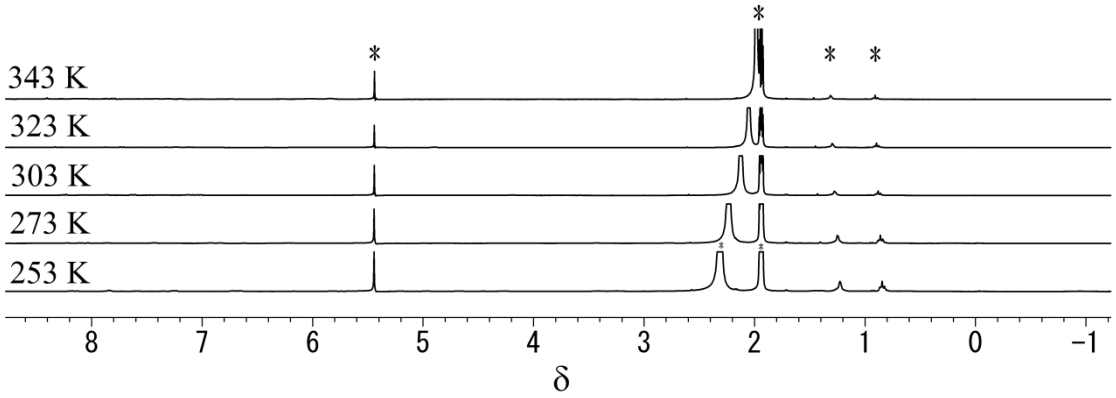

Figure S9. Variable temperature ^{1}H NMR spectra (300 MHz) of complex **4** in acetonitrile-d_3. Residual solvent signals are marked with an asterisk.

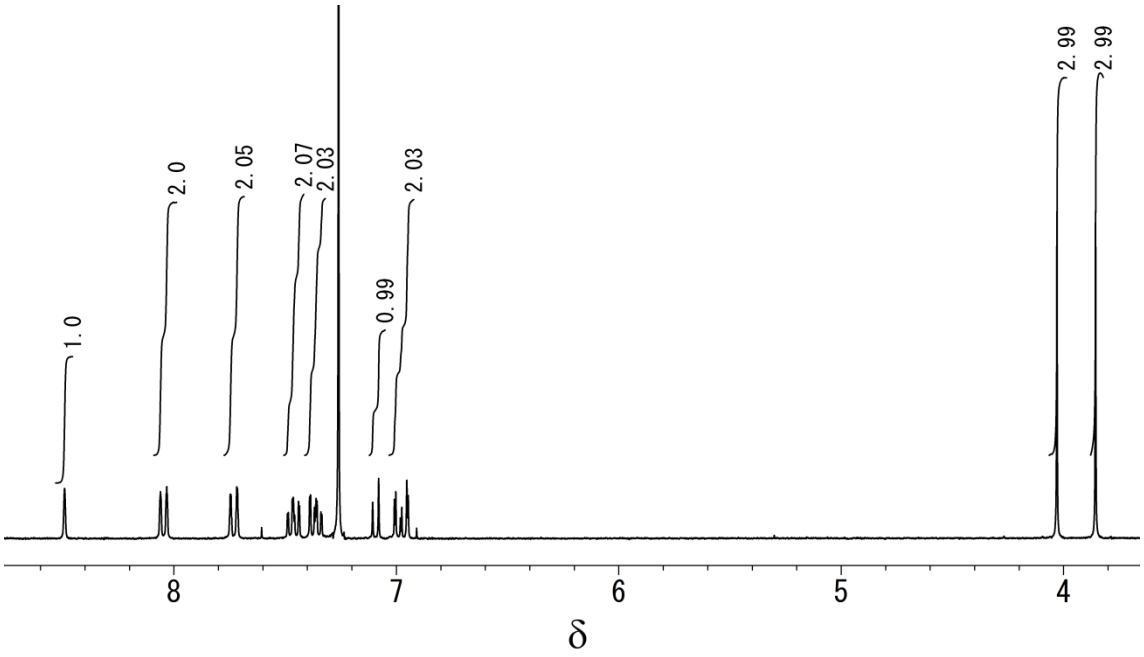

Figure S10. ^{1}H NMR spectrum (300 MHz, $CDCl_3$) of **(i)**.

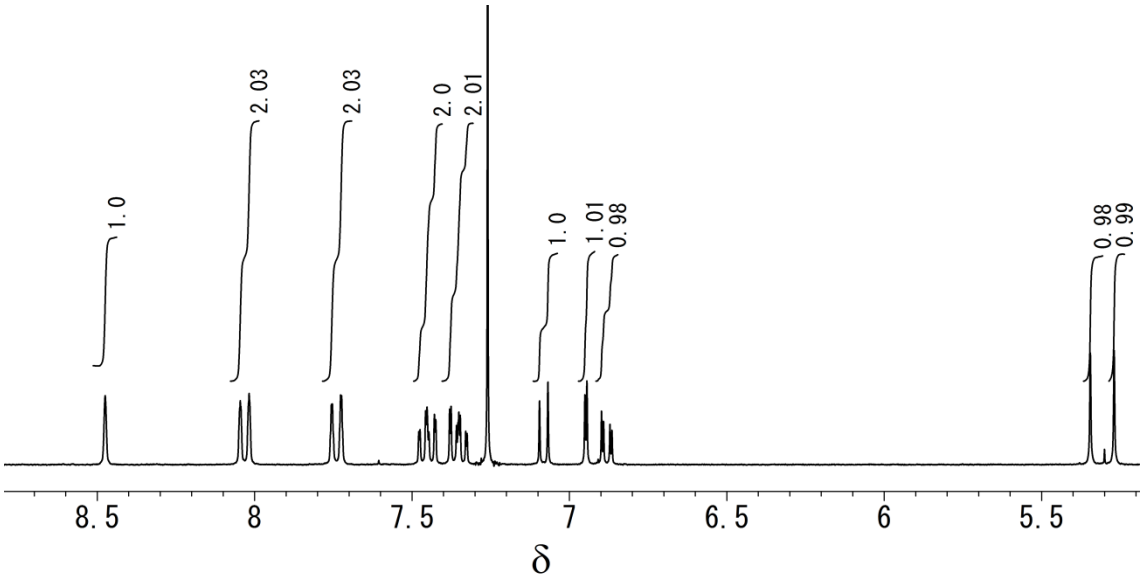

Figure S11. ^{1}H NMR spectrum (300 MHz, $CDCl_3$) of H_2L.